Electronic Supplementary Information

Karst landform-featured monolithic electrode for water electrolysis in neutral media

Xueqing Gao,[a] Yingdong Chen,[a] Tong Sun,[b] Jianmei Huang,[c] Wei Zhang,*[a] Qiang Wang*[c] and Rui Cao*[ad]

[a]Key Laboratory of Applied Surface and Colloid Chemistry, Ministry of Education; School of Chemistry and Chemical Engineering, Shaanxi Normal University, Xi'an 710119, China

[b]Bruker (Beijing) Scientific Technology Co., Ltd, Beijing 100192, China

[c]College of Chemistry and Molecular Engineering, Nanjing Tech University, Nanjing 211816, China

[d]Department of Chemistry, Renmin University of China, Beijing 100872, China

*Corresponding authors:

zw@snnu.edu.cn (W.Z.); ruicao@ruc.edu.cn (R.C.); wangqiang@njtech.edu.cn (Q.W.)

General materials

All reagents, including nickel foam (thickness: 1.7 mm, area density: 380 mg cm^{-2}, Lizhiyuan Co.), H_2SO_4 (98%, Sinopharm Chemicals), HCl (38%, Sinopharm Chemicals), $NaH_2PO_4 \cdot 2H_2O$ (99.99%, Alfa), Na_2HPO_4 (99.99%, Alfa), Pt/C catalysts (20 wt%, E-TEK), Ir/C (20 wt%, Premetek Co.), ethanol (99.7%, Sinopharm Chemicals), and Nafion (5 wt%, DuPont) were purchased from commercial suppliers and used without further purification. Natural seawater was collected in the Yellow Sea of China. Milli-Q water of 18 MΩ cm was used in all experiments unless otherwise stated.

Table S1. A summary of the electrocatalytic water splitting performance of various bifountional electrocatalysts in near neutral aqueous solution.

Catalyst	Electrolyte	η (mV) of HER	η (mV) of OER	Water electrolysis	References
Karst NF	**1.0 M PBS (pH = 7)**	**110 @10 mA cm^{-2}**	**432 @10 mA cm^{-2}**	**1.88 V @10 mA cm^{-2}**	**This work**
Karst NF	**1.0 M PBS (pH = 7)**	**190 @10 mA cm$^{-2}_{ECSA}$**	**648 @10 mA cm$^{-2}_{ECSA}$**	–	**This work**
Karst NF	**Seawater (pH = ~8)**	–	–	**1.79 V @10 mA cm^{-2}**	**This work**
CoCat	0.5 M KPi* (pH = 7) 0.1 M KPi** (pH = 7)	435* @2 mA cm^{-2}	400** @1 mA cm^{-2}	–	**Nat. Mater.*, 2012, **11**, 802-807; ***Science*, 2008, **321**, 1072-1075.
NiCat	0.1 M NaBi (pH = 9.2)	670 @3 mA cm^{-2}	870 @2 mA cm^{-2}	–	*J. Phy Chem. C*, 2014, **118**, 4578-4584.
Co-P-B/rGO	0.1 M PBS (pH = 7)	640 @10 mA cm^{-2}	400 @10 mA cm^{-2}	–	*J. Mater. Chem. A*, 2014, **2**, 18420-18427.
CoO/$CoSe_2$	0.5 M PBS (pH = 6.86)	337 @10 mA cm^{-2}	510 @10 mA cm^{-2}	2.18 V @10 mA cm^{-2}	*Adv. Sci.*, 2016, **3**, 1500426.
CoOx/CN	1.0 M KPi (pH = 7)	280 @10 mA cm^{-2}	300 @10 mA cm^{-2}	–	*J. Am. Chem. Soc.*, 2015, **137**, 2688-2694.
Ni_3Se_4/Ni	1.0 M PBS (pH = 7)	269 @10 mA cm^{-2}	480 @10 mA cm^{-2}	–	*ACS Appl. Mater. Interfaces*, 2017, **9**, 8714-8728.
ONPPGC/OCC	0.2 M PBS (pH = 7)	~520 @2 mA cm^{-2}	~550 @10 mA cm^{-2}	1.71 V @2 mA cm^{-2}	*Energy Environ. Sci.*, 2016, **9**, 1210-1214.

η: overpotential; −: data not available; PBS: phosphate buffered saline; KPi: potassium phosphate buffer; NaBi: sodium borate buffer; CN: N-doped carbon hybrids; ONPPGC/OCC: The oxygen, nitrogen and phosphorus tri-doped porous graphite carbon@oxidized carbon cloth.

Table S2. Comparison of HER performance of Karst NF and other 3D-electrodes with separate active sites in near neutral aqueous solution.

Catalyst	Substrate	Electrolyte	η (mV) of HER	References
Karst NF	**NF**	**1.0 M PBS (pH = 7)**	**110 @10 mA cm^{-2}**	**This work**
Ni_3S_2/NF	NF	1 M KPi (pH = 7)	170 @10 mA cm^{-2}	*J. Am. Chem. Soc.*, 2015, **137**, 14023-14026.
CoP-MNA	NF	0.5 M PBS (pH = ~7)	~172 @10 mA cm^{-2}	*Adv. Funct. Mater.*, 2015, **25**, 7337-7347.
S-$NiFe_2O_4$/NF	NF	1.0 M PBS (pH = 7.4)	197 @10 mA cm^{-2}	*Nano Energy*, 2017, **40**, 264-273.
CoO/$CoSe_2$	Ti mesh	0.5 M PBS (pH = 6.86)	337 @10 mA cm^{-2}	*Adv. Sci.*, 2016, **3**, 1500426.
FeP NAs/CC	carbon cloth	1 M PBS (pH = 7)	202 @10 mA cm^{-2}	*ACS Catal.*, 2014, **4**, 4065-4069.
$FeMoS_4$ NRA/CC	carbon cloth	1.0 M PBS (pH = 7)	204 @10 mA cm^{-2}	*Chem. Commun.*, 2017, **53**, 9000-9003.
$CoMoS_4$ NS/CC	carbon cloth	1.0 M PBS (pH = 7)	183 @10 mA cm^{-2}	*Nano Res.*, 2018, **11**, 2024-2033.
Ni-Mo-S/C	carbon fiber cloth	0.5 M NaPi (pH = 6.9)	200 @10 mA cm^{-2}	*Sci. Adv.*, 2015, **1**, e1500259.

η: overpotential; PBS: phosphate buffered saline; KPi: potassium phosphate buffer; NaPi: sodium phosphate buffer; CoP-MNA: CoP mesoporous nanorod arrays; FeP NAs/CC: FeP nanorod arrays on carbon cloth; $FeMoS_4$ NRA/CC: $FeMoS_4$ nanorod array on carbon cloth; $CoMoS_4$ NS/CC: $CoMoS_4$ nanosheet array on carbon cloth.

Table S3. Comparison of OER performance of Karst NF and other 3D-electrodes with separate active sites in near neutral aqueous solution.

Catalyst	Substrate	Electrolyte	η (mV) of HER	References
Karst NF	**NF**	**1.0 M PBS (pH = 7)**	**432 @10 mA cm^{-2}**	**This work**
Ni_3Se_4/Ni	NF	1.0 M PBS (pH = 7)	480 @10 mA cm^{-2}	*ACS Appl. Mater. Interfaces*, 2017, **9**, 8714-8728.
S-$NiFe_2O_4$/NF	NF	1 M PBS (pH = 7)	494 @10 mA cm^{-2}	*Nano Energy*, 2017, **40**, 264-273.
CoO/$CoSe_2$	Ti mesh	0.5 M PBS (pH = 6.86)	510 @10 mA cm^{-2}	*Adv. Sci.*, 2016, **3**, 1500426.
Co-Bi/Ti	Ti mesh	0.1 M KBi (pH = 9.2)	469 @10 mA cm^{-2}	*J. Mater. Chem. A*, 2017, **5**, 7305-7308.
Co@Co-Bi/Ti	Ti mesh	0.4 M NaBi (pH = ~9)	470 @10 mA cm^{-2}	*Nanoscale*, 2017, **9**, 16059-16065.
Co-Pi NA	Ti mesh	0.1 M PBS (pH = 7)	450 @10 mA cm^{-2}	*Angew. Chem. Int. Ed.*, 2017, **56**, 1064-1068.
CCH@Co-Pi NA/Ti	Ti mesh	0.1 M PBS (pH = 7)	460 @10 mA cm^{-2}	*Nanoscale*, 2017, **9**, 3752-3756.
Ni-Bi/CC	carbon cloth	0.1 M KBi (pH = 9.2)	470 @10 mA cm^{-2}	*Chem. Commun.*, 2017, **53**, 3070-3073.

η: overpotential; PBS: phosphate buffered saline; KBi: potassium borate buffer; NaBi: sodium borate buffer; Co@Co-Bi/Ti: cobalt borate nanosheets grown on metallic cobalt deposited on Ti-mesh; Co-Pi NA: cobalt phosphate nanoarray; CCH@Co-Pi NA/Ti: $Co(CO_3)_{0.5}(OH)\cdot 0.11H_2O$@Co-Pi nanoarray on Ti mesh.

Table S4. A summary of The ECSA values of Ni, α-$Ni(OH)_2$ of the karst NF and their proportion after different electrolysis time.

Karst NF (cm^2)				
		after HER		
		2 h	10 h	205 h
α-$Ni(OH)_2$	0.84	0.65	0.52	0.19
Ni	0.77	0.96	1.09	1.42
α-$Ni(OH)_2$: Ni	1.1	0.68	0.48	0.13
		after OER		
		2 h	10 h	205 h
α-$Ni(OH)_2$	0.84	1.10	1.30	1.45
Ni	0.77	0.51	0.31	0.16
α-$Ni(OH)_2$: Ni	1.1	2.16	4.19	9.06

Table S5. A summary of our photovoltaic-electrolysis seawater splitting performance and various reported water electrolysis cells for alkaline water splitting.

water electrolysis cell	Electrolyte Solution	η_{STE}	η_{ETH}	η_{STH}	References
karst NF || karst NF	**Seawater**	**25.5%**	**64.7%**	**16.5%**	**This work**
NiFe LDH || NiFe LDH	1 M NaOH	17.3%	~71.1%	12.3%	*Science*, 2014, **345**, 1593-1596.
CoMnO@CN || CoMnO@CN	1 M KOH	16.1%	~49.7%	8%	*J. Am. Chem. Soc.*, 2015**, 137**, 14305-14312.
NiFeSP/NF || NiFeSP/NF	1 M KOH	28.5%	~32.3%	9.2%	*ACS Nano*, 2017, **11**, 10303-10312.
Ni-NPs@NC || FeNi@N-CNT	1 M KOH	20%	~53%	10.6%	*ACS Appl. Mater. Interfaces*, 2016, **8**, 35390-35397.

η_{STE}: solar-to-electric conversion efficiency; η_{ETH}: electric-to-hydrogen conversion efficiency; η_{STH}: solar-to-hydrogen conversion efficiency; NF: nickel foam; LDH: layered double hydroxides; CN: N-doped carbon; NC: N-doped carbon structure; N-CNT: N-doped carbon nanotube.

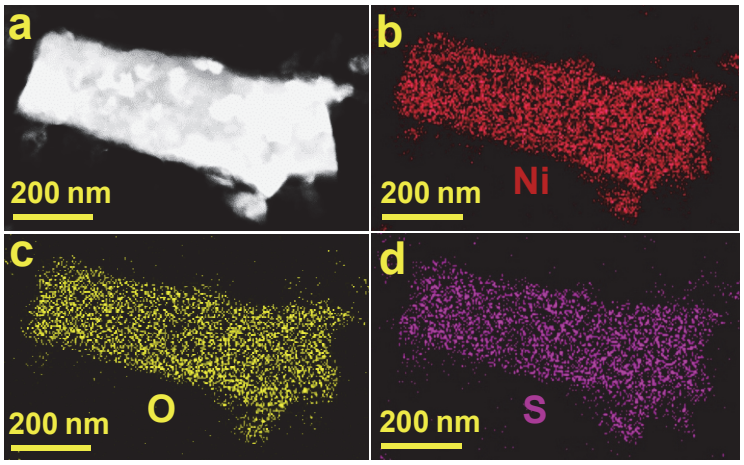

Fig. S1 (a) The HAADF STEM image and (b-d) the corresponding EDX elemental mappings of the tower in karst NF.

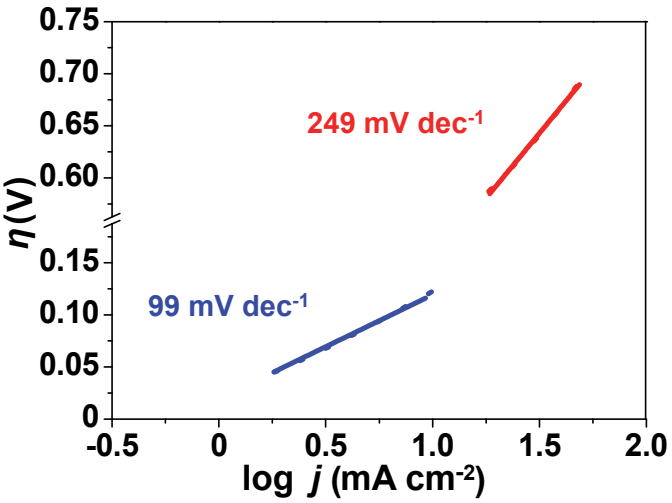

Fig. S2 Tafel plots for HER (blue) and OER (red) of the karst NF in 1.0 M pH = 7 PBS .

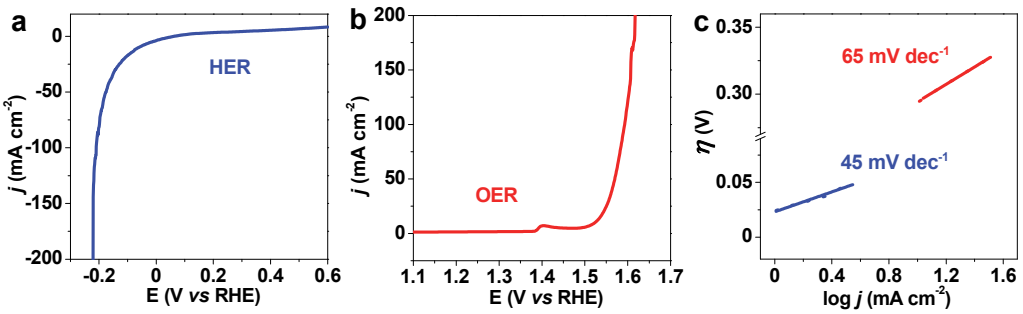

Fig. S3 Electrocatalytic (a) HER and (b) OER performance of karst NF in a 1.0 M KOH. (c) Tafel plots for HER (blue) and OER (red) of karst NF in a 1.0 M KOH.

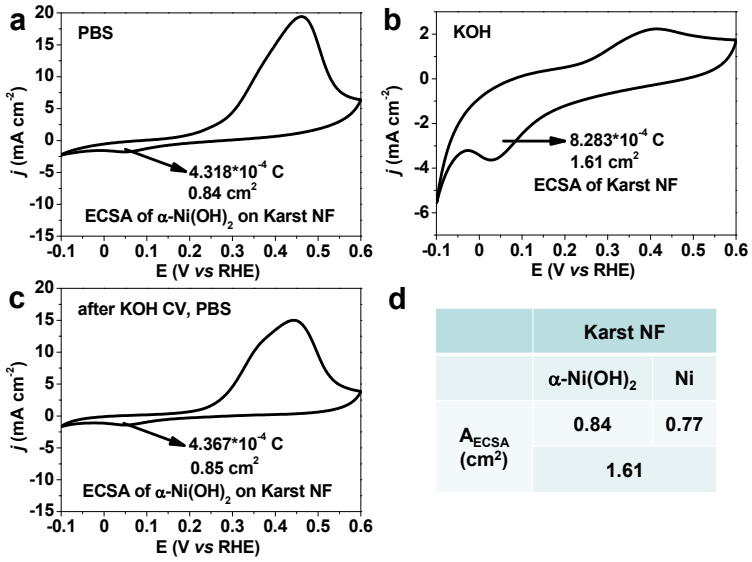

d

	Karst NF	
	α-Ni(OH)$_2$	Ni
A_{ECSA} (cm^2)	0.84	0.77
	1.61	

Fig. S4 CVs for the karst NF scanned from 0.6 to −0.1 V(*vs* RHE) at a sweep rate of 50 mV s^{-1} in (a) 1 M PB, (b) 1 M NaOH and (c) 1 M PB by sequence. (d) The ECSA values of Ni, α-$Ni(OH)_2$, and the karst NF.

The charge for the formation of a monolayer α-$Ni(OH)_2$ is 514 μC cm^{-2}.[*J. Mater. Chem., 2012, 22, 15153*] The reduction peak at 0~0.1 V corresponds to the reduction of $Ni(OH)_2$ to Ni.[*Adv. Mater. 2019, 1806296; Energy Environ. Sci., 2013, 6, 1509*] In order to obtain the initial amount of α-$Ni(OH)_2$ on the surface, a karst NF electrode was first scanned from 0.6 to −0.1 V (*vs* RHE) in 1 M phosphate buffer (PB). The reduction peak area was referred to estimate the ECSA of α-$Ni(OH)_2$ on karst NF (Fig S4a). Then, to obtain the total amount of active Ni and α-$Ni(OH)_2$ on the surface of karst NF from an one monolayer of OH adsorption on karst NF, the OH desorption region in 1 M NaOH was used to estimate the ECSA of karst NF (Fig S4b). The ECSA of surface Ni can thus be obtained by $ECSA_{Ni} = ECSA_{karstNF} - ECSA_{\alpha\text{-}Ni(OH)_2}$. Last, the karst NF electrode was re-scanned from 0.6 to −0.1 V (vs RHE) in 1 M PB. The $ECSA_{\alpha\text{-}Ni(OH)_2}$ (Fig S4c) is almost the same as the obtained value in Fig S4a, which proved that this method is reliable. The ECSA values are summarized in Fig. S4d.

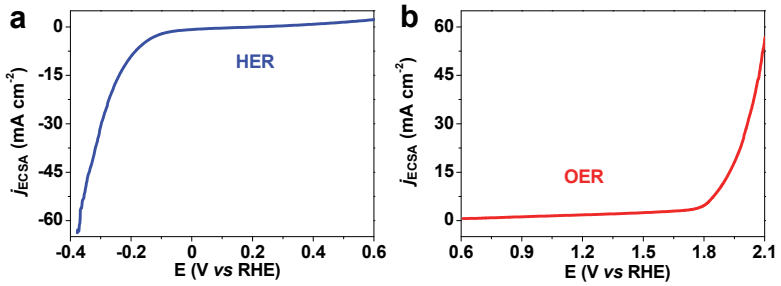

Fig. S5 Polarization curves for HER and OER (normalized to the ECSAs) in a 1.0 M pH = 7 PBS.

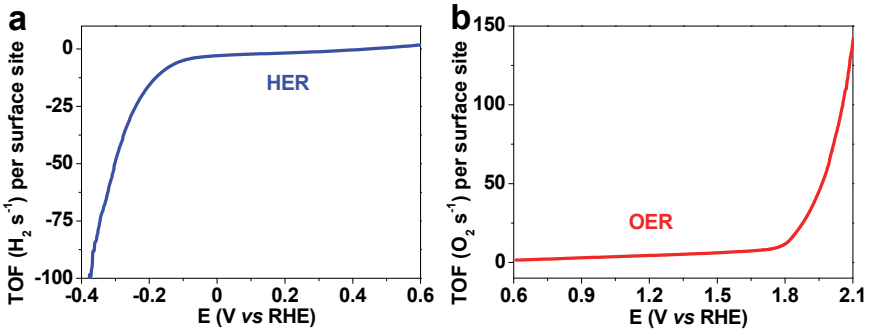

Fig. S6 TOF plots for (a) HER and (b) OER of the karst NF in 1.0 M pH = 7 PBS.

TOF values were calculated according to the following formula:

$$\text{TOF} = \frac{\text{Number of total } H_2 \text{ (or } O_2\text{) turnovers per second / geometric area } \left(\text{cm}^2\text{s}^{-1}\right)}{\text{Number of active sites / geometric area } \left(\text{cm}^2\right)}$$

Number of total H_2 (or O_2) turnovers can be calculated based on the current density (j) according to:

$$\text{Number of } H_2 = j\left(\frac{\text{mA}}{\text{cm}^2}\right) \times \frac{1\text{ C s}^{-1}}{1000\text{ mA}} \times \frac{1\text{ mol e}^-}{96485.3\text{ C}} \times \frac{1\text{ mol } H_2}{2\text{ mol e}^-} \times \frac{6.022\times10^{23}\ H_2\ \text{molecules}}{1\text{ mol } H_2}$$

$$= j\left(\frac{\text{mA}}{\text{cm}^2}\right) \times 3.12\times10^{15}\ H_2\ \text{molecules}\left(\frac{\text{s}^{-1}}{\text{mA}}\right)$$

$$\text{Number of } O_2 = j\left(\frac{\text{mA}}{\text{cm}^2}\right) \times \frac{1\text{ C s}^{-1}}{1000\text{ mA}} \times \frac{1\text{ mol e}^-}{96485.3\text{ C}} \times \frac{1\text{ mol } O_2}{4\text{ mol e}^-} \times \frac{6.022\times10^{23}\ O_2\ \text{molecules}}{1\text{ mol } O_2}$$

$$= j\left(\frac{\text{mA}}{\text{cm}^2}\right) \times 1.56\times10^{15}\ O_2\ \text{molecules}\left(\frac{\text{s}^{-1}}{\text{mA}}\right)$$

Note that we use the number of surface Ni^{2+} sites for OER, and the number of surface Ni sites for HER, respectively.

The active sites per real surface area is calculated from the following formula:

$$\text{Number of active sites} = \left(\frac{\text{Number of atoms / unit cell}}{\text{Volume / unit cell}}\right)^{\frac{2}{3}}$$

The crystal structure of Ni and α-$Ni(OH)_2$ are shown below:

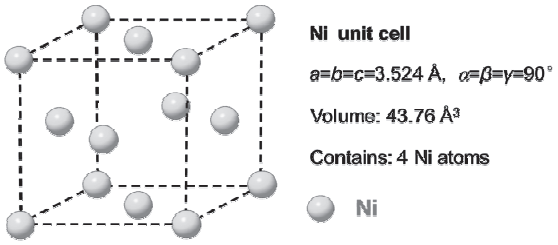

Ni unit cell

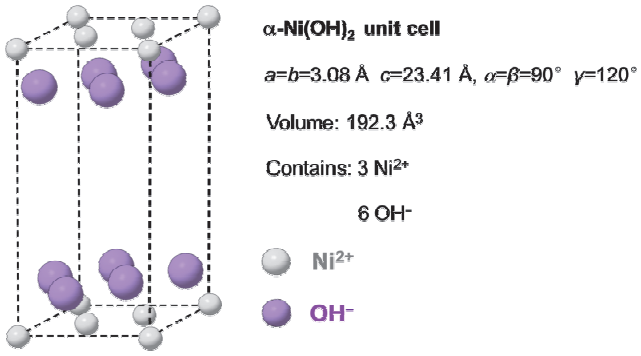

α-Ni(OH)$_2$ unit cell

$$\text{Number of active sites (Ni)} = \left(\frac{4 \text{ atoms / unit cell}}{43.76 \text{ Å}^3 \text{ / unit cell}}\right)^{\frac{2}{3}} = 2.03\times10^{15} \text{atoms cm}^{-2}$$

$$\text{Number of active sites } (\alpha\text{-Ni(OH)}_2) = \left(\frac{3 \text{ atoms / unit cell}}{192.3 \text{ Å}^3 \text{ / unit cell}}\right)^{\frac{2}{3}} = 0.624\times10^{15} \text{atoms cm}^{-2}$$

Finally, the TOF can be calculated as:

$$\text{TOF}_{\text{HER}} = \frac{j(\frac{\text{mA}}{\text{cm}^2})\times 3.12\times10^{15}\ \text{H}_2\ \text{molecules}\ (\frac{\text{s}^{-1}}{\text{mA}})\times \text{A}_{\text{geo}}(\text{cm}^2)}{\text{Number of active sites } (\text{cm}^{-2})\times\ \text{A}_{\text{ECSA}}(\text{cm}^2)}$$

$$= \frac{j(\frac{\text{mA}}{\text{cm}^2})\times 3.12\times10^{15}(\frac{\text{s}^{-1}}{\text{mA}})\times 0.25(\text{cm}^2)}{2.03\times10^{15}(\text{cm}^{-2})\times\ 0.77(\text{cm}^2)} = 0.499\,j(\text{s}^{-1})$$

$$\text{TOF}_{\text{OER}} = \frac{j(\frac{\text{mA}}{\text{cm}^2})\times 1.56\times10^{15}\ \text{O}_2\ \text{molecules}\ (\frac{\text{s}^{-1}}{\text{mA}})\times \text{A}_{\text{geo}}(\text{cm}^2)}{\text{Number of active sites } (\text{cm}^{-2})\times \text{A}_{\text{ECSA}}(\text{cm}^2)}$$

$$= \frac{j(\frac{\text{mA}}{\text{cm}^2})\times 1.56\times10^{15}(\frac{\text{s}^{-1}}{\text{mA}})\times 0.25(\text{cm}^2)}{0.624\times10^{15}(\text{cm}^{-2})\times\ 0.84(\text{cm}^2)} = 0.744\,j(\text{s}^{-1})$$

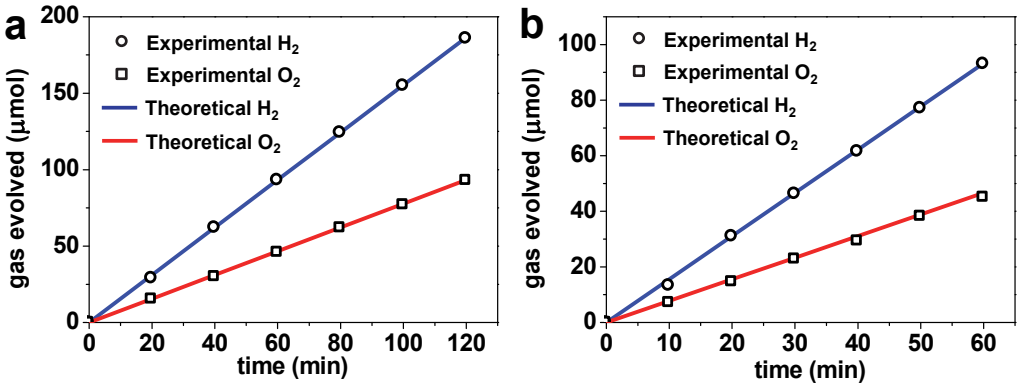

Fig. S7 Experimental (from gas chromatography analysis) and theoretical (from transferred charge) amounts of H_2 and O_2 evolved during water electrolysis from the karst NF||karst NF cell in (a) 1.0 M pH = 7 PBS and (b) seawater.

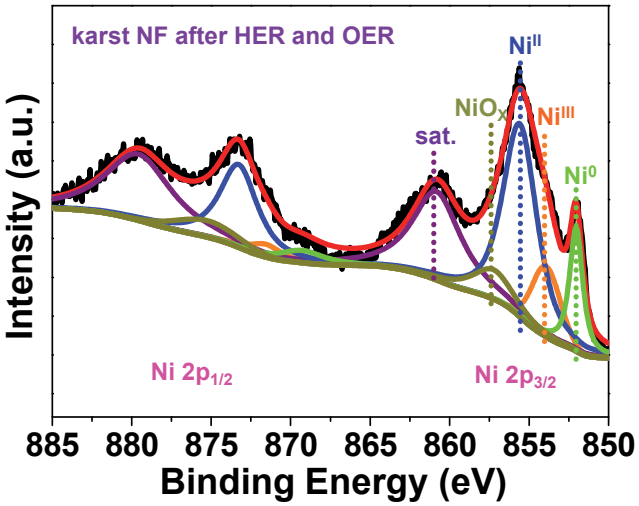

Fig. S8 Narrow scan XPS spectrum near the Ni 2p binding energy region after the polarization switches between HER (−0.21 V, 2h, no iR compensation) and OER (1.91 V, 2h, no iR compensation) tests.

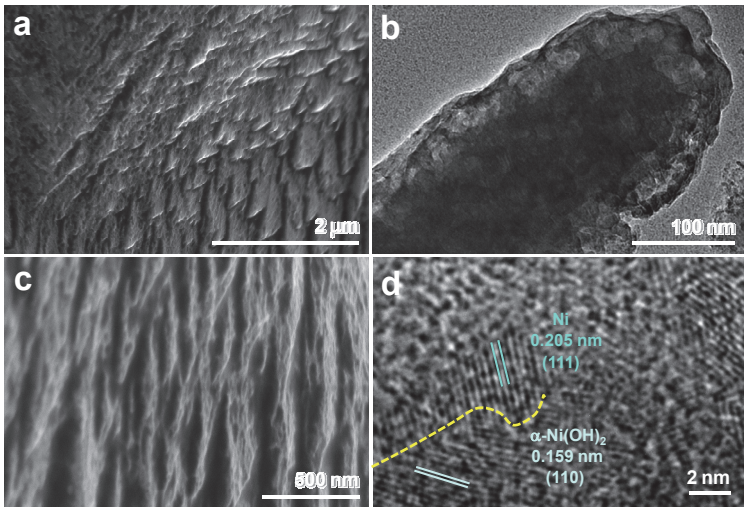

Fig. S9 (a,c) SEM and (b,d) TEM images of the karst NF after switched HER and OER durability tests.

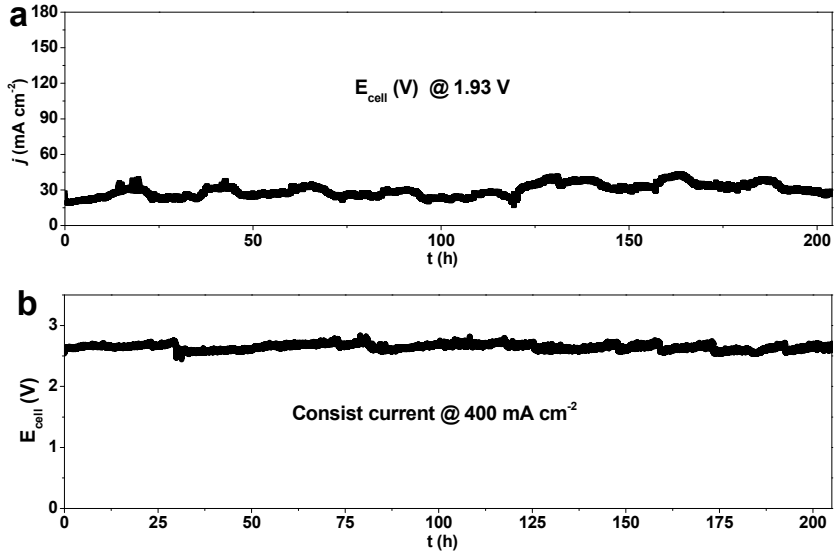

Fig. S10 (a) Long-term chronoamperometry stability test (>200 h) of karst NF||karst NF cell in 1.0 M pH = 7 PBS at 1.93 V. (b) Long-term chronopotentiometry stability test (>200 h) of karst NF||karst NF cell 1.0 M pH = 7 PBS under an industrial-required current density of 400 mA cm^{-2}.

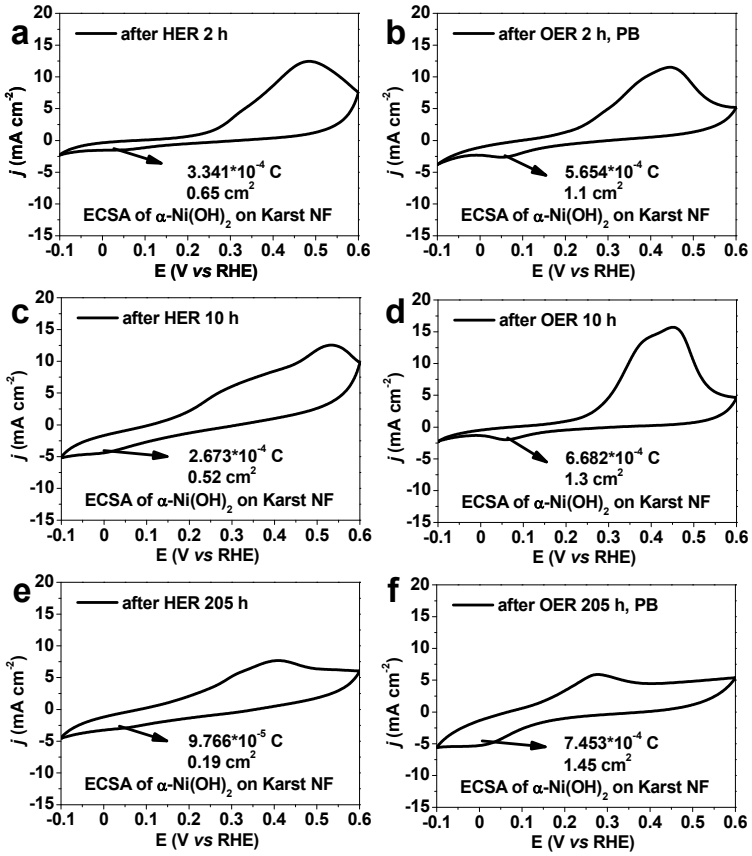

Fig. S11 CVs for the karst NF scanned from 0.6 to −0.1 (V vs RHE) in 1.0 M PBS after different electrolysis time.

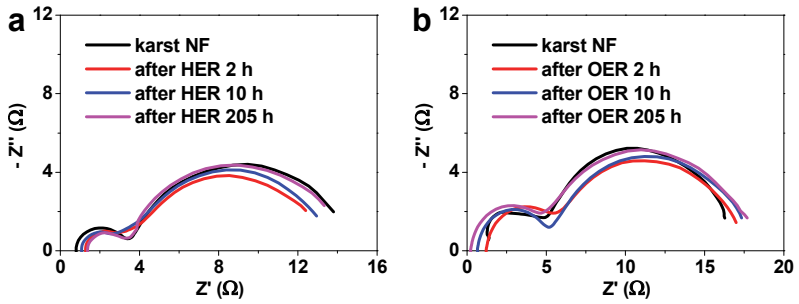

Fig. S12 Nyquist plots of the karst NF at different times for HER and OER tests.

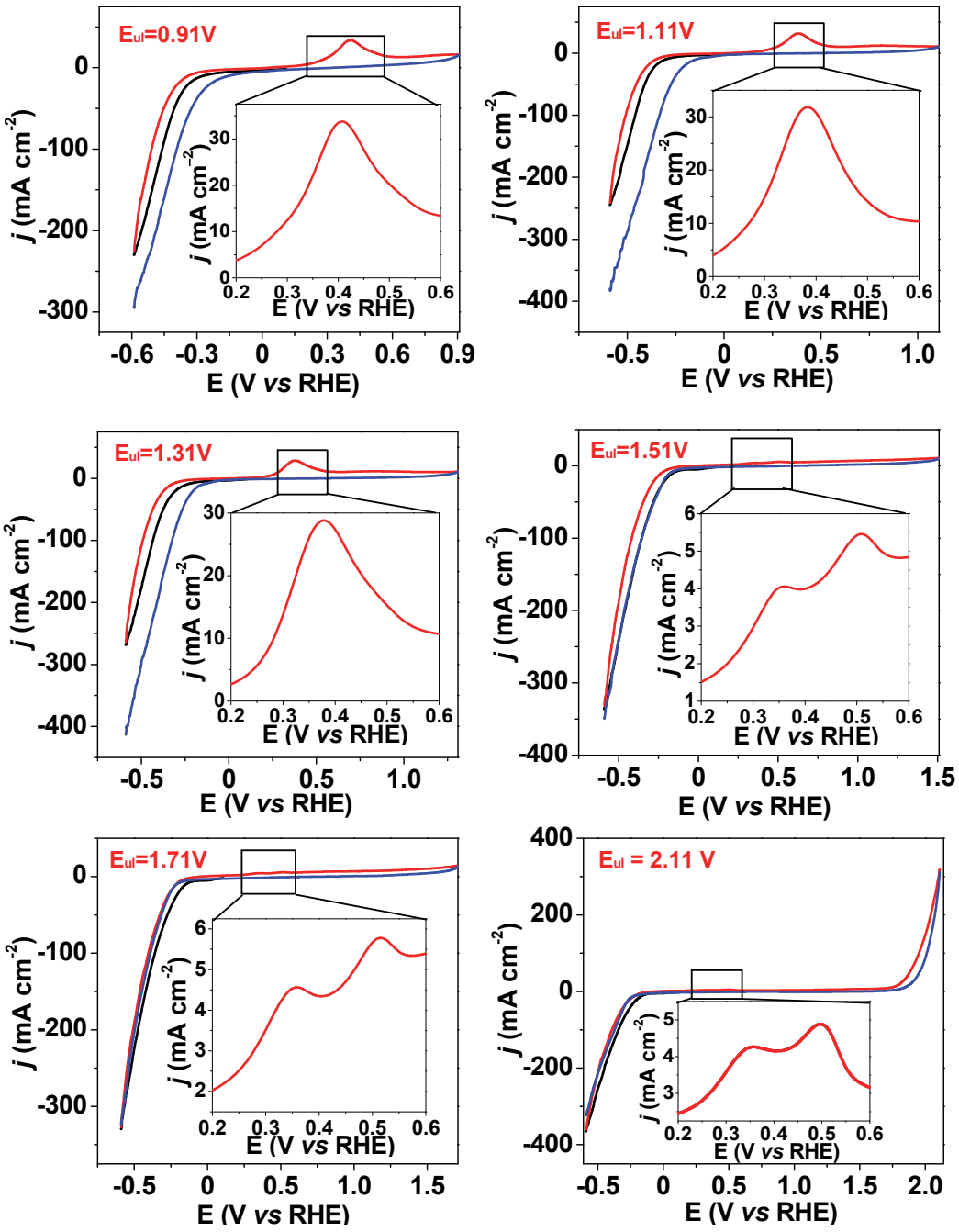

Fig. S13 CVs of the karst NF at E_{ul} = 0.91, 1.11, 1.31, 1.51, 1.71 and 2.11 V with enlarged regions from 0.2 to 0.6 V (inset).

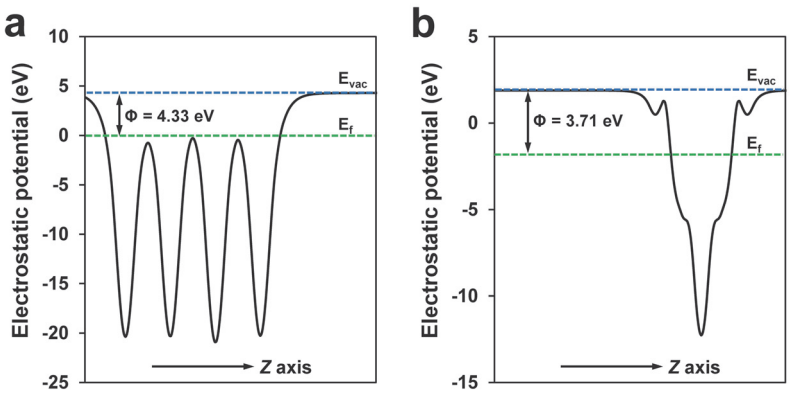

Fig. S14 The electrostatic potential calculations of (a) Ni metal and (b) $Ni(OH)_2$. The blue and green dash lines represent the vacuum (E_{vac}) and Fermi level (E_f) potentials, respectively. The difference between the two levels is the work function.

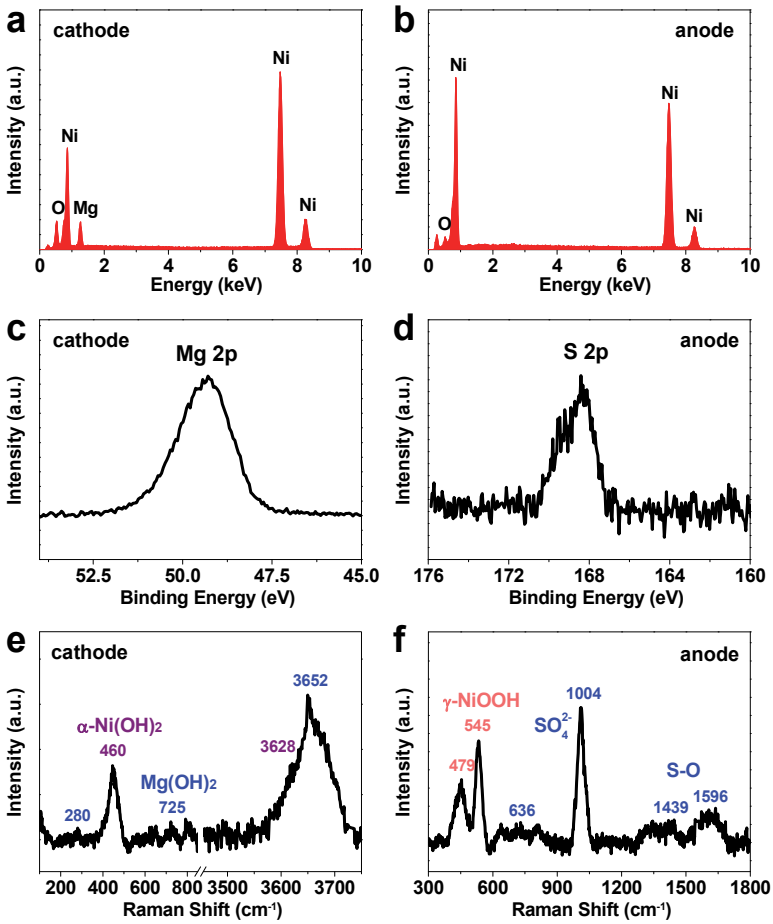

Fig. S15 Spectral characterizations of the karst NF electrodes after water splitting in natural seawater: (a, b) EDX spectra, (c, d) narrow scan XPS spectra and (e, f) Raman spectra.

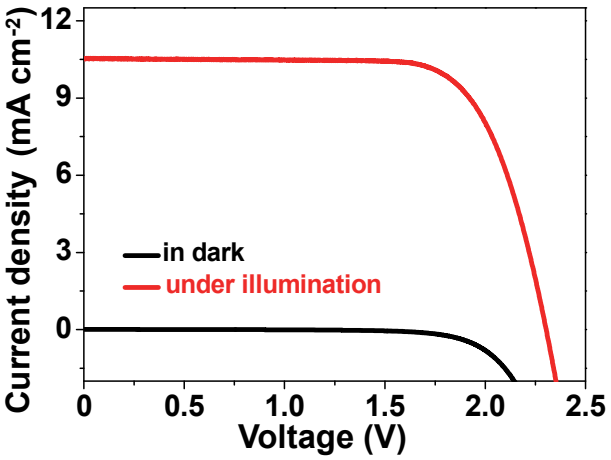

Fig. S16 Current-voltage curve of a commercial Si planar solar cell with an open-circuit voltage of 2.3 V and a photo-current conversion efficiency of 25.5%.